ELSEVIER

Surface Science 478 (2001) L327–L332

SURFACE SCIENCE

www.elsevier.nl/locate/susc

Surface Science Letters

Photon emission from individual supported gold clusters: thin film versus bulk oxide

N. Nilius *, N. Ernst, H.-J. Freund

Department of Chemical Physics, Fritz-Haber-Institut der Max-Planck-Gesellschaft, Faradayweg 4-6, D-14195 Berlin, Germany

Received 11 January 2001; accepted for publication 5 February 2001

Abstract

To examine effects of different substrates (Al_2O_3/NiAl and TiO_2) on electronic properties of single, selected Au particles we have measured electron-stimulated photon emission spectra using a scanning tunneling microscope. An assignment is made to collective electronic excitations (Mie plasmons) in supported Au clusters which is suggested by model calculations. Plasmon lifetimes, derived from homogenous line widths, are considerably shorter for Au on Al_2O_3/NiAl (1.8 fs) than for Au/TiO_2 (4.7 fs).

Keywords: Scanning tunneling microscopy; Photon emission; Plasmons; Clusters; Surface electronic phenomena (work function, surface potentials, surface states, etc.)

Thin oxide films, grown on metal substrates, play an important role as supports for studies of the physical and chemical properties of model catalysts [1–3]. Their small thickness allows the application of electron and ion mediated surface science methods without charging problems. For processes, dominated by short range interactions, a similar behavior has been found on thin films and bulk oxides (adsorption, diffusion, metal adhesion) [1–3]. On the other hand, little is known about the screening ability of long range interactions in thin oxide films. An electromagnetic coupling to the underlying metal substrate can influence the electronic properties of small metal aggregates, deposited on oxide films. The efficiency of the effect can be determined via the lifetime of specific electronic excitations, which can be deduced from homogenous line widths by employing the uncertainty relation $\Gamma_{\mathrm{hom}}\tau \geqslant 2\hbar$. Because of large oscillator strengths, collective electronic excitations in small metal aggregates represent promising candidates to examine the correlation between cluster–substrate interaction and excitation lifetime [4].

Plasmon modes have been observed in light absorption [4–7], differential reflection [8] and electron energy loss (EEL) spectroscopy [9], but can also be detected via the light emission following a radiating decay [10–12]. Intrinsic decay channels, such as dielectric losses and electron-surface scattering events [4–6,13], and substrate mediated channels [4–6,14] contribute to the plasmon lifetime in the metal particle. Two mechanisms of substrate induced damping are conceivable [4]: (i) electron transfer from the cluster into 'affinity

* Corresponding author. Tel.: +49-30-8413-4316; fax: +49-30-8413-4306.

E-mail address: nilius@fhi-berlin.mpg.de (N. Nilius).

0039-6028/01/$ - see front matter
PII: S0039-6028(01)00951-7

levels' of the surrounding medium destroying the phase coherence of the collective oscillation; (ii) coupling to electronic excitations in the support. For ensembles of embedded Ag clusters, the reduction of the plasmon lifetime with increasing cluster–substrate interaction has been demonstrated [5]. However, the determination of the homogeneous line width, reflecting the plasmon lifetime in a single cluster, is complicated by inhomogeneous line broadening effects due to the cluster-size distribution in the sample. This difficulty can be circumvented by employing optical spectroscopies on individual particles. In this way, the light absorption of single Au clusters has been measured in an optical nearfield microscope [15]. Using electron-stimulated photon emission in a scanning tunneling microscope (PSTM) [16], we have recently characterized Mie resonances in individual, oxide supported Ag clusters [12]. To improve our understanding of cluster–substrate interactions, we would like to present comparative PSTM measurements on Au clusters, prepared on Al_2O_3 thin films and bulk TiO_2. Gold clusters have primarily been chosen, because their Mie plasmon energy is significantly smaller than the band gaps of both oxides.

In our experiment, photon emission from an individual cluster was stimulated by electron injection from the tip of an STM. The tip was positioned above the cluster, selected after taking a topographic image of the sample surface. At tip voltages below ± 15 V (tip–sample distance <4 nm), the diameter of the electron beam was smaller than the mean cluster–cluster distance to ensure excitation of a single cluster. Photons emitted after excitation of the cluster were collected by a parabolic mirror surrounding the STM. After passing a quartz window the light was focused on the slit of a grating spectrograph and detected with a CCD camera. The STM setup was mounted in an UHV chamber (base pressure $p < 2 \times 10^{-10}$ mbar) equipped with standard techniques for sample preparation and analysis [17]. A $TiO_2(1\,1\,0)$ surface and a thin Al_2O_3 film were used as supports in the experiments. To ensure sufficient conductivity of the TiO_2 single crystal, the sample was annealed to 1000 K for 10 min in UHV. The induced oxygen release creates free electrons in the conduction band of the oxide, followed by a change of its color from transparent to blue [18]. Alternating Ar sputtering and annealing cycles to 800 K produced a clean $TiO_2(1\,1\,0)$ surface, characterized by a sharp (2×1) LEED pattern. The corresponding STM image is dominated by a pattern of parallel white lines (Fig. 1a). The observed topographic structure is compatible with an added row model of Ti_2O_3 stripes [19]. The alumina film was prepared by exposing a clean $NiAl(1\,1\,0)$ surface to 1000 L of O_2 at 600 K. Subsequent annealing of the sample to 1300 K leads to the formation of a thin, well ordered alumina film, showing sharp LEED spots. The thickness of the film had been estimated to 0.5 nm, thus being highly transparent for low energy electrons, but sufficiently thick to determine the growth mode of the gold [3]. An STM image shows the specific defect structure of the film, dominated by boundaries between two types of oxide domains (Fig. 1b) [3]. Au particles were prepared at room temperature by atom deposition from the gas phase, followed by diffusion and nucleation to three-dimensional clusters. On titania (Fig. 1c) step edges are preferential nucleation centers. On the alumina film (Fig. 1d), Au

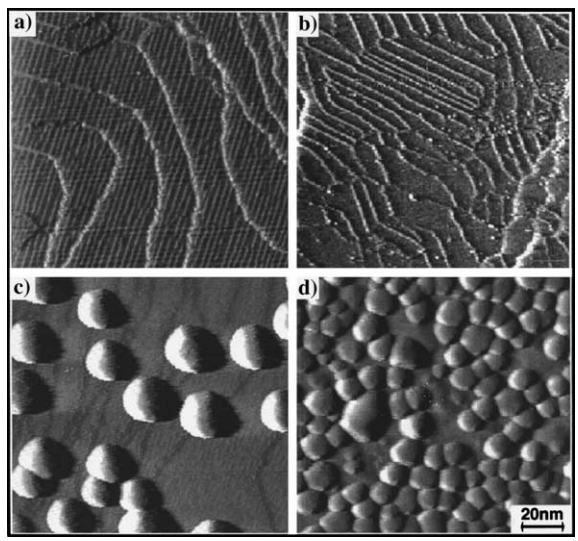

Fig. 1. STM images of (a) $TiO_2(1\,1\,0)$, (b) $Al_2O_3/NiAl(1\,1\,0)$, (c) $Au/TiO_2(1\,1\,0)$ and (d) $Au/Al_2O_3/NiAl(1\,1\,0)$. Cluster diameters are broadened due to tip convolution effects.

nucleates additionally at oxide domain boundaries, thus giving a higher cluster density.

Photon emission spectra of Au clusters have been obtained at identical experimental conditions on both substrates (accumulation time: 500 s, electron current: 2 nA). Au clusters of similar dimensions (diameter 7 nm, height 4 nm) were selected to avoid size effects on the emission characteristics. Modifications of the cluster shape were ruled out through imaging the surface before and after each spectroscopic run.

On clean $TiO_2(1\,1\,0)$ no photon emission is observed, whereas electron injection into an Au cluster causes an intense emission line at 2.22 eV with a full width at half maximum (FWHM) of 0.28 ± 0.02 eV (Fig. 2a). This homogenous line width corresponds to a minimum lifetime of 4.7 fs. An increase of tip bias, implying a retraction of the tip from the surface, leads to an intensity loss and a peak shift to 2.25 eV. Reversing the polarity leaves the peak position unchanged. However, the light intensity emitted from an Au cluster, is considerably reduced and decreases faster with tip bias for positive than for negative polarity. In Fig. 2b, the data on the bottom show a photon emission spectrum of the clean alumina film, governed by a single peak at 1.3 eV. Its width is artificially narrowed due to the sensitivity cut-off of the light detector at 1.1 eV. The emission is caused by a radiating decay of tip induced plasmons (TIP) in the W-tip/NiAl tunnel junction, excited due to the strong electromagnetic coupling between tip and sample in an STM [20]. The thin alumina film covering the NiAl metal substrate does not change the emission characteristics of the TIP. Positioning the tip above an Au cluster gives an additional emission peak at 2.50 eV in the spectra. The line width of 0.72 ± 0.05 eV ($\tau = 1.8$ fs) is considerably broadened compared to Au particles on TiO_2. As for Au on bulk TiO_2, a decreasing intensity and a slight blue shift of the peak to 2.53 eV are observed at higher negative tip bias for Au on the Al_2O_3 film. The 2.5 eV emission line from small Au clusters can hardly be detected for positive polarity. A summary of the optical properties of Au particles is given in Table 1.

To explain the present experimental results, two photon emission mechanisms are conceivable. The presence of the STM tip in close proximity to the cluster makes an emission process following the concept of a TIP very likely [21]. Thereby, the strong electromagnetic interaction between tip and sample causes collective oscillations of the electron gas in tip and sample, driven by the inelastic part of the tunnel current. An intensity loss of the emission for increasing tunnel bias is predicted as

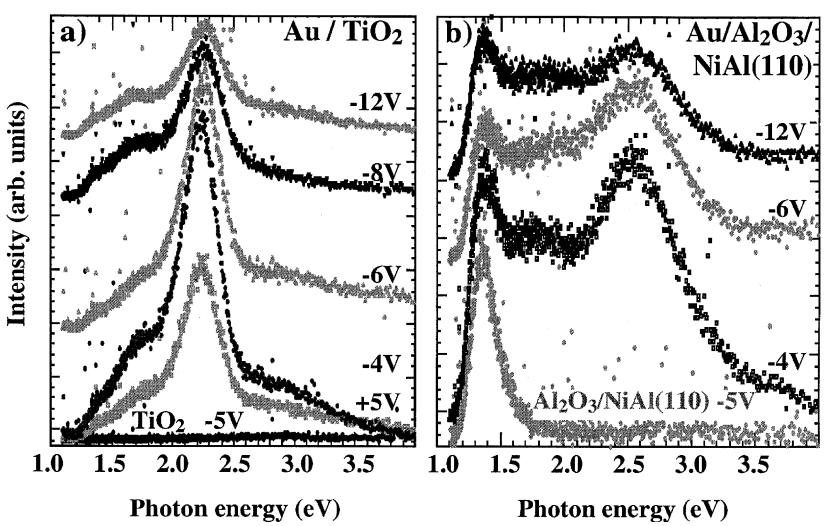

Fig. 2. Photon emission spectra of individual Au clusters (diameter 7 nm, height 4 nm) on (a) $TiO_2(1\,1\,0)$ and (b) Al_2O_3/NiAl(1 1 0) taken at 2 nA electron current.

Table 1
Resonance positions, line widths and lifetimes for Mie plasmons in Au clusters

Substrate	$TiO_2(1\,1\,0)$[a]		$Al_2O_3/NiAl$[a] (Exp.)	Al_2O_3[a] (Theo.)	NiAl[a] (Theo.)	In TiO_2[b] (Exp.)	In Al_2O_3[c] (Exp.)
	(Exp.)	(Theo.)					
$\hbar\omega$ (eV)	2.25	2.30	2.53	2.40	2.50	1.9	2.37
FWHM (eV)	0.28	0.25	0.72	0.35	0.39	0.16	0.39
τ (fs)	4.7	–	1.8	–	–	8	–

[a] This work.
[b] Single clusters [15].
[c] Cluster ensemble [13].

result of a reduced coupling at larger tip–sample distances. However, in contrast to theoretical expectations, photon emission from Au clusters was observed at high voltages and large tip–sample separations. For emission spectra taken at −12 V tip bias and 3 nm tip–sample separation (Fig. 2a and b, data on top), the cross-section of a TIP based photon emission process should be low. Additionally, differences in the emitted light intensity for positive and negative bias are not consistent with the TIP model. Assuming similar tunneling conditions for both polarities, the excitation probability of an interface plasmon should be independent of the direction of the electron current, which was not observed.

In an alternate approach, the light emission is treated as an intrinsic property of the Au particles, neglecting the tip influence on the actual photon emission process. The emission is now interpreted as a radiating decay of collective electronic oscillations in the Au cluster (Mie plasmons) excited after electron bombardment [4]. At present experimental conditions, oscillations perpendicular to the substrate plane (1,0 mode) can exclusively be excited, because electrons from the tip are injected along the surface normal. In this model, the decrease of light intensity at increasing bias and tip–sample distances results from the expanding size of the electron beam spot. A growing fraction of electrons from the tip misses the cluster, which leads to a smaller plasmon-excitation probability. Also, the reduced emission intensity at positive tip bias becomes understandable. At positive bias, electrons leaving the cluster are accelerated in the electric field towards the tip. In close proximity to the cluster, their energy gain is not yet sufficient to excite a plasmon. For opposite polarity, field emitted electrons from the tip have maximum energy when injected into the cluster and can easily provide the plasmon excitation energy. The small blueshift of the gold-related emission line, observed at increasing tip bias, indicates a slight tip influence on the emission process. However, in the case of large tip–sample separations the polarizability of the coupled tip–cluster system is dominated by the cluster and the tip weakly affects the energetic position of the plasmon [22]. Differences in the emission behavior of Au particles on TiO_2 and $Al_2O_3/NiAl$ cannot be explained by intrinsic cluster properties, since clusters of almost identical size and shape have been selected for the spectroscopic analyses. They have rather to be interpreted as a consequence of different cluster–substrate interactions. Therefore, the presence of the tip is neglected in the following calculation to account for a realistic description of the cluster polarizability and cluster–substrate interactions.

In the theoretical approach, developed in the group of Jupille [23], the polarizability of a truncated spheroid on a substrate is determined in a nonretarded limit. Cluster and substrate materials enter the calculation through their complex dielectric functions (Au, TiO_2, NiAl [24–26]). A multipole expansion is used for the electromagnetic potentials in cluster, substrate and vacuum, whereby the localization of the cluster–multipoles is not fixed in its center. Image multipoles are included to describe cluster–substrate interactions. By solving the Laplace equation for all potentials under a weak formulation of boundary conditions, the electronic polarizability of the spheroid is derived. The result is transferred into an effective

dielectric function of the metal particle, ε_{cl}, which is used to calculate the electron energy loss (EEL) probability, P of an electron injected into the spheroid [27]:

$$P \propto (\varepsilon_{substrate}+1)^{-2}\mathrm{Im}(\varepsilon_{cl}) + (\varepsilon_{substrate})^{2}(\varepsilon_{substrate}+1)^{-2}\mathrm{Im}(-1/\varepsilon_{cl}).$$

The simulation is restricted to electron stimulated excitation processes in the cluster; subsequent decay mechanisms of electronic excitations are not included. Since radiating decay channels compete with nonradiating mechanisms, deviations between calculated EEL probabilities and observed emission spectra have to be considered. Fig. 3a shows the energy dependence of the EEL probability for electrons injected into an Au particle on a TiO_2 surface. Cluster size and shape were adapted to experimental conditions. The calculated spectrum is dominated by a maximum in the EEL probability at 2.3 eV, which corresponds to the excitation of the perpendicular mode of the Mie plasmon. The measured emission peak is slightly lower in energy. This could be the consequence of ignoring the interaction of the Mie plasmon with its image dipole in the STM tip. A parallel orientation of the two dipoles lowers the energy of the coupled system and shifts the plasmon frequency to lower values. In the experiment, this tip influence is detected as a small redshift of the emission line for decreasing bias and tip–sample separations. The width of the resonance (FWHM = 0.25 eV) is approximately reproduced in the simulation. The value is close to the expected FWHM for Au particles in vacuum, demonstrating the marginal influence of the TiO_2 support on the plasmon lifetime. Because of the 3.1 eV band gap neither 'affinity levels' for a temporary transfer of excited electrons nor empty states for electronic excitations are available in TiO_2 in the relevant energy range. Nevertheless, a previously measured FWHM (0.16 eV) of the plasmon absorption line in individual Au particles embedded in TiO_2 [15] is considerably smaller than our value (0.28 eV). The reason becomes obvious from the shift of the plasmon frequency to 1.9 eV due to the complete enclosure of the cluster in the dielectric matrix. At this energy the imaginary part of the Au dielectric function is noticeably smaller and dielectric losses inside the particle are reduced. The remaining EEL intensity on the high energy side of the plasmon resonance in Fig. 3a reflects the energy absorption due to interband transitions in gold above 2.5 eV, not observed in the emission spectroscopy.

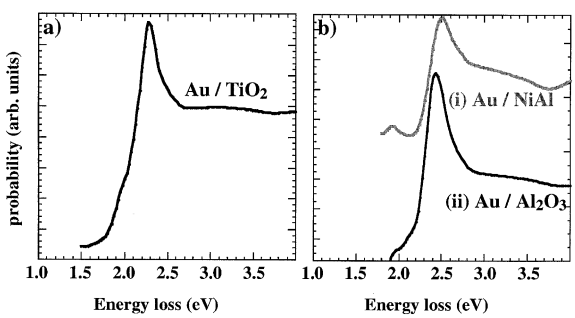

Fig. 3. Calculated EEL spectra for electrons injected into Au spheroids (diameter 7 nm, height 4 nm) on: (a) TiO_2, (b) NiAl (curve (i)) and Al_2O_3 (curve (ii)).

The calculation of the EEL probability of Au on Al_2O_3 show distinct differences to experimental results (Fig. 3b, curve(ii)). Naturally, the emission peak at 1.3 eV, assigned to the TIP mode in the NiAl/W tunnel cavity, cannot be reproduced in a model neglecting the STM tip. The reduced polarizability of alumina compared to titania shifts the Mie plasmon to higher energies in agreement with experiment. Nevertheless, neither the experimentally determined peak position nor the FWHM of the resonance is reproduced in the model. Obviously, an oxide film of 0.5 nm is not thick enough to screen the plasmon excitation in the Au particle from the NiAl substrate. The electric nearfield associated with the oscillating dipole in the cluster penetrates into the metal and couples to electronic excitations in NiAl.

To model the experimental situation in a more realistic manner, the Au spheroid was directly placed on the NiAl crystal, neglecting the thin alumina film (Fig. 3b, curve(i)). The electromagnetic interaction of the Mie plasmon with the metallic substrate further shifts the resonance towards the measured position of 2.53 eV. The calculated line width is broadened to 0.39 eV due to the onset of Au interband transitions. The underestimation

of the FWHM compared to the experimental result of 0.72 eV is a specific problem of the calculation, which cannot account for a substrate induced decay mechanism of the plasmon. Whereas for insulators with sufficiently large band gaps this decay channel can be neglected, it plays a major role in the present case of a metallic support. The dielectric loss function of NiAl shows a distinct maximum at 2.5 eV, being exactly the energetic position of the Au Mie resonance [26]. This maximum can be correlated with transitions from NiAl d-bands to empty s,p orbitals above the Fermi level [28]. The additional line broadening of the plasmon resonance measured for Au particles on Al_2O_3/NiAl is therefore explained by the occurrence of an efficient energy transfer from the plasmon excitation to interband transitions in NiAl.

In conclusion, we have compared photon emission processes for Au clusters supported on bulk TiO_2 and a thin Al_2O_3 film. Stimulating the light emission with the tip of an STM, optical properties of individual clusters could be studied without inhomogeneous line broadening effects due to the cluster size distribution. Calculations of the dynamic polarizability of Au particles favor an assignment of the emission to the radiating decay of Mie plasmons. The line width of the plasmon resonance measured for an individual Au cluster on TiO_2 is close to the expected value for Au clusters in vacuum, indicating a weak cluster–substrate interaction. In contrast, the Au plasmon resonance experiences a large broadening when the cluster is deposited on a thin Al_2O_3 film on NiAl(1 1 0). The strong electromagnetic coupling between collective excitations in the Au particle and interband transitions in the NiAl is discussed as the origin for a reduced plasmon lifetime.

Acknowledgements

For using the program code of the calculation we are grateful to R. Lazarri and J. Jupille. The work was supported by the Deutsche Forschungsgemeinschaft, the Fond der Chemischen Industrie and the NEDO Research Grant on Photon and Electron Controlled Surface Processes.

References

[1] C.T. Campbell, Surf. Sci. Rep. 27 (1997) 3.
[2] C.R. Henry, Surf. Sci. Rep. 31 (1998) 231.
[3] M. Bäumer, H.-J. Freund, Progr. Surf. Sci. 61 (1999) 127.
[4] U. Kreibig, W. Vollmer, Optical Properties of Metal Clusters, Vol. 25, Springer Series Materials Science, Springer, Berlin, 1995.
[5] H. Hövel, S. Fritz, A. Hilger, U. Kreibig, M. Vollmer, Phys. Rev. B 48 (1993) 18178.
[6] K.-P. Charlé, L. König, S. Nepijko, I. Rabin, W. Schulze, Cryst. Res. Technol. 33 (1998) 1085.
[7] T. Wenzel, J. Bosbach, F. Stietz, F. Träger, Surf. Sci. 432 (1999) 257.
[8] D. Martin, J. Jupille, Y. Borensztein, Surf. Sci. 402 (1998) 433.
[9] C.-M. Grimaud, L. Siller, M. Andersson, R.E. Palmer, Phys. Rev. B 59 (1999) 9874.
[10] T. Kume, S. Hayashi, K. Yamamoto, Phys. Rev. B 55 (1997) 4774.
[11] A. Downes, M.E. Welland, Appl. Phys. Lett. 72 (1998) 2671.
[12] N. Nilius, N. Ernst, H.-J. Freund, Phys. Rev. Lett. 84 (2000) 3994.
[13] R. Antoine, M. Pellarin, B. Palpant, M. Broyer, B. Prével, P. Galletto, P.F. Brevet, H.H. Girault, J. Appl. Phys. 84 (1998) 4532.
[14] J.-Y. Bigot, J.-C. Merle, O. Cregut, A. Daunois, Phys. Rev. Lett. 75 (1995) 4702.
[15] T. Klar, M. Perner, S. Grosse, G.v. Plessen, W. Spirkl, J. Feldmann, Phys. Rev. Lett. 80 (1998) 4249.
[16] R. Berndt, in: R. Wiesendanger (Ed.), Scanning Probe Microscopy, Springer Series, Nanoscience and Technol., Springer, Berlin, 1998, p. 97.
[17] N. Nilius, A. Cörper, G. Bozdech, N. Ernst, H.-J. Freund, Prog. Surf. Sci. 67 (2001).
[18] R. Hasiguti, Adv. Mater. Sci. 2 (1972) 69.
[19] H. Onishi, Y. Iwasawa, Phys. Rev. Lett. 76 (1996) 791.
[20] N. Nilius, N. Ernst, P. Johansson, H.-J. Freund, Phys. Rev. B 61 (2000) 12682.
[21] P. Johansson, R. Monreal, P. Apell, Phys. Rev. B 42 (1990) 9210.
[22] A. Downes, M.E. Taylor, M.E. Welland, Phys. Rev. B 57 (1998) 6706.
[23] I. Simonsen, R. Lazzari, J. Jupille, S. Roux, Phys. Rev. B 61 (2000) 7722.
[24] E.D. Palik (Ed.), Handbook of Optical Constants of Solids, Academic Press, Orlando, 1985.
[25] G. Fuentes, I. Mancheno, F. Balbas, C. Quiros, J.F. Trigo, F. Yubero, E. Elizalde, J.M. Sanz, Phys. Stat. Sol. 175 (1999) 429.
[26] H. Jacobi, R. Stahl, Z. Metallkde 60 (1969) 106.
[27] H. Lüth, Surfaces and Interfaces of Solids, Springer, Berlin, 1993.
[28] D.J. Peterman, R. Rosei, D.W. Lynch, V.L. Moruzzi, Phys. Rev. B 21 (1980) 5505.